Synthetic Route to Nanocomposites Made Up of Inorganic Nanoparticles Confined within a Hollow Mesoporous Carbon Shell

Antonio B. Fuertes,*,† Marta Sevilla,† Teresa Valdes-Solis,† and Pedro Tartaj‡

Instituto Nacional del Carbón (CSIC), Apartado 73, 33080, Oviedo, Spain, and Instituto de Ciencia de Materiales de Madrid (CSIC), Cantoblanco, 28049, Madrid, Spain

Received June 27, 2007. Revised Manuscript Received September 4, 2007

We present here a novel and simple synthetic strategy for fabricating core/shell materials (diameter ∼400 nm) made up of inorganic nanoparticles confined within a hollow mesoporous carbon shell (shell thickness ∼50 nm). This methodology has been applied to the encapsulation of a variety of inorganic phases such as Fe_3O_4/γ-Fe_2O_3, $CoFe_2O_4$, $LiCoPO_4$, NiO, and Cr_2O_3. An important characteristic of these core/shell composites is that, whereas the inner macroporous core can be almost completely filled by nanoparticles, the porosity of the carbon shell hardly contains deposited nanoparticles. In consequence, these materials exhibit large surface areas (∼500−700 $m^2 \cdot g^{-1}$), high pore volumes (∼0.3−0.6 $cm^3 \cdot g^{-1}$), and a porosity made up of accessible pores of ∼2−2.5 nm. We demonstrated the usefulness of these composites for the immobilization of an enzyme (lysozyme) and proved their easy manipulation by means of an external magnetic field.

Introduction

Hollow particles, also referred to as capsules, have recently attracted great attention because they can be used in emergent applications, such as drug delivery vehicles, highly efficient catalysts, core/shell composites, dye encapsulation, or immobilization of biomolecules.[1] These materials have the unique feature of providing a protected core suitable for encapsulating a large variety of substances. Liposomes, nanoengineered polyelectrolyte multilayer microcapsules, or micelles are typical examples of capsules. Recently, capsules composed of a macroporous core and a mesoporous inorganic shell have also generated considerable interest.[2] The advantages of porous inorganic capsules are that they combine a high surface area and a large mesopore volume with a good chemical inertness and mechanical stability. They may be used to fabricate functional materials made up of nanoparticles confined within macroporous cores or deposited in the porous layer of the capsule. What is more, if we could design these hollow-core/shell nanocomposites so that they have sizes in the colloidal range, we could expand their processing capabilities.[3] A few examples of these nanocomposites have already been reported in the literature.[4]

Our interest has focused on designing colloidal hollow-core/shell nanocomposites made up of inorganic nanoparticles confined within a carbon shell containing nonobstructed pores. Here we present a novel approach for encapsulating inorganic substances within the macroporous core of mesoporous carbon colloidal capsules. A core/shell system with these structural properties has important advantages. First, the performance of such encapsulated nanoparticles in many applications can be enhanced because the carbon shell acts as a barrier that prevents their coalescence. An example of this is the use of encapsulated Pt nanoparticles as high-performance catalysts, as reported by Ikeda and co-workers.[5] Second, the external carbon layer ensures a good electrical conductivity, which is essential for many applications related with the electrochemical use of poor conductive encapsulated inorganic materials (i.e., electroactive materials in Li-ion batteries). Third, the mesoporous carbon shell will allow the rapid diffusion of reactants/products (this is important when the core is filled with a nanocatalyst) or electrolytes (this is

* Corresponding author. E-mail: abefu@incar.csic.es.
† Instituto Nacional del Carbón (CSIC).
‡ Instituto de Ciencia de Materiales de Madrid (CSIC).

(1) (a) Caruso, F.; Trau, D.; Mohwald, H.; Renneberg, R. *Langmuir* **2000**, *16*, 1485. (b) Caruso, F. *Adv. Mater.* **2001**, *13*, 11. (c) Kim, S.-W.; Kim, M.; Lee, W. Y.; Hyeon, T. *J. Am. Chem. Soc.* **2002**, *124*, 7642. (d) Lesieur, S.; Grabielle-Madelmont, C.; Menager, C.; Cabuil, V.; Dadhi, D.; Pierrot, P.; Edwards, K. *J. Am. Chem. Soc.* **2003**, *125*, 5266. (e) Tartaj, P.; Morales, M.; Veintemillas-Verdaguer, P. S.; Gonzalez-Carreño, T.; Serna, C. J. *J. Phys. D: Appl. Phys.* **2003**, *36*, R182. (f) Lavan, D. A.; Mcguire, T. *Nat. Biotechnol.* **2003**, *21*, 1184. (g) Ren, N.; Dong, A.-G.; Cai, W.-B.; Zhang, Y.-H.; Yang, W.-L.; Huo, S.-J.; Chen, Y.; Xie, S. H.; Gao, Z.; Tang, Y. *J. Mater. Chem.* **2004**, *14*, 3548. (h) Sukhorukov, G. B.; Rogach, A. L.; Zebli, B.; Liedl, T.; Skirtach, A. G.; Kçhler, K.; Antipov, A. A.; Gaponik, N.; Susha, A. S.; Winterhalter, M.; Parak, W. J. *Small* **2005**, *1*, 194. (i) Skirtach, A. G.; Muñoz-Javier, A.; Kreft, O.; Köhler, K.; Piera-Alberola, A.; Möhwald, H.; Parak, W. J.; Sukhorukov, G. B. *Angew. Chem., Int. Ed.* **2006**, *45*, 4612. (j) Johnston, A. P. R.; Cortez, C.; Angelatos, A. S.; Caruso, F. *Curr. Opin. Colloid Surf. Sci.* **2006**, *11*, 203.

(2) (a) Yoon, S. B.; Sohn, K.; Kim, J. Y.; Shin, C. H.; Yu, J. S.; Hyeon, T. *Adv. Mater.* **2002**, *14*, 19. (b) Wang, J. W.; Xia, Y. D.; Wang, W. X.; Mokaya, R.; Poliakoff, M. *Chem. Commun.* **2005**, 210. (c) Yu, J. S.; Yoon, S. B.; Lee, Y. J.; Yoon, K. B. *J. Phys. Chem. B* **2005**, *109*, 7040. (d) Im, S. H.; Jeong, U.; Xia, Y. *Nat. Mater.* **2005**, *4*, 671. (e) Yoon, S. B.; Kim, J. Y.; Kim, J. H.; Park, S. G.; Lee, C. W.; Yu, J. S. *Curr. Appl. Phys.* **2006**, *6*, 1059. (f) Lee, J.; Kim, J.; Hyeon, T. *Adv. Mater.* **2006**, *18*, 2073.

(3) (a) Ozin, G. A. *Chem. Commun.* **2003**, 2639. (b) López, C. *Adv. Mater.* **2003**, *15*, 1679.

(4) (a) Kim, M.; Sohn, K.; Na, H.; Hyeon, T. *Nano Lett.* **2002**, *2*, 1383. (b) Kim, J. Y.; Yoon, S. B.; Yu, J. S. *Chem. Commun.* **2003**, 790. (c) Chai, G. S.; Yoon, S. B.; Kim, J. H.; Yu, J. S. *Chem. Commun.* **2004**, 2766.

(5) (a) Ikeda, S.; Ishino, S.; Harada, T.; Okamoto, N.; Sakata, T.; Mori, H.; Kuwabata, S.; Torimoto, T.; Matsumura, M. *Angew. Chem., Int. Ed.* **2006**, *45*, 7063. (b) Ng, Y. H.; Ikeda, S.; Harada, T.; Higashida, S.; Sakata, T.; Mori, H.; Matsumura, M. *Adv. Mater.* **2007**, *19*, 597.

10.1021/cm071713k CCC: $37.00
Published on Web 10/05/2007

Table 1. Structural Properties of the Core/Shell Composites[a]

sample	synthesis conditions temperature/time (atmosphere: N_2)	nanoparticle size (nm)[b]	textural properties		
			S_{BET} ($m^2 \cdot g^{-1}$)	V_p ($cm^3 \cdot g^{-1}$)	pore size (nm)[c]
CS−Fe_xO_y	260 °C/2 h	14	590	0.47	2.1
CS−$CoFe_2O_4$	280 °C/2 h	9	690	0.55	2.5
CS−$LiCoPO_4$	600 °C/1 h	>30	400	0.32	1.9
CS−NiO	300 °C/1 h	3	520	0.45	2.1
CS−Cr_2O_3	500 °C/6 h	12	490	0.40	1.9

[a] The percentage of inorganic phase in these composites is around 50 wt %, except for the CS−$LiCoPO_4$ sample that contains 60 wt % of lithium cobalt phosphate. [b] Obtained by means of the Scherrer equation applied to the XRD peaks. [c] Maximum of the pore size distribution.

crucial when the core is loaded with an electroactive substance) between the outer surface of the particle and the substance confined inside the core of the capsule. Fourth, the partial filling of the macroporous core of the capsule with magnetic nanoparticles will allow the magnetic manipulation (i.e., extraction from or transport through a liquid medium) of large molecules (biomolecules) adsorbed onto the mesoporous carbon shell and/or confined in the core.

The techniques usually employed to fabricate core/shell nanocomposites normally entail first the synthesis of the nanoparticles to be encapsulated and then the growing of a coating layer (normally of silica or carbon).[6] These procedures are somewhat complex and involve a multistep process. Moreover, they give rise to core/shell nanocomposites that in most cases contain only a few nanoparticles confined inside the macroporous core (nanorattles).[4a,4b,5,6b,6e] Alternatively, other methods based on aerosol techniques that are continuous and easily scaleable lead to materials with a nonpermeable shell.[7] The synthetic strategy reported in this paper has two important advantages: (a) the macroporous core of the carbon capsules can be filled with a significant number of inorganic nanoparticles as opposed to by only a few of them,[5] and (b) this methodology can be used to encapsulate a variety of inorganic materials. Finally, to demonstrate the potential of these materials, we examined the immobilization of an enzyme over a core/shell magnetic nanocomposite obtained using this novel synthetic strategy.

Experimental Section

Preparation of (Inorganic Core)/(Porous Carbon Shell) Nanocomposites. Carbon capsules with a macroporous hollow core and a mesoporous shell were prepared by using submicrometric solid core/mesoporous shell silica spheres[8] as sacrificial templates according to the procedure reported by Yoon et al.[2a] To incorporate the inorganic phase into the macroporous hollow core, the carbon capsules were impregnated with a solution of inorganic precursor dissolved in ethanol. This solution was added dropwise until incipient wetness, and then the impregnated sample was dried at 80 °C. This process was repeated several times until the desired amount of inorganic precursor was attained (currently ∼50% of the inorganic phase in the composite). The inorganic precursors employed were the corresponding metal nitrates used to obtain Fe_xO_y, $CoFe_2O_4$, NiO, and Cr_2O_3. The formula Fe_xO_y denotes the magnetic iron oxides with an inverse cubic spinel structure, which comprise both magnetite (Fe_3O_4) and maghemite (γ-Fe_2O_3). The magnetic properties of these iron oxides are very similar. Maghemite only differs from magnetite in that all the Fe cations are in the trivalent state. Because it is very difficult to discern, from the XRD patterns, the exact crystalline phase (magnetite or maghemite) present in the iron oxide ferrite nanoparticles, we used the general formula Fe_xO_y. In the case of $LiCoPO_4$ we employed a mixture of LiH_2PO_4 and cobalt nitrate dissolved in water. All the products were purchased from Aldrich. To convert the impregnated inorganic precursor into the desired inorganic phase we used different procedures. NiO, Cr_2O_3, and $LiCoPO_4$ were obtained by a simple thermal treatment under nitrogen atmosphere at the conditions listed in Table 1. The nanoparticles of ferrites (Fe_xO_y and $CoFe_2O_4$) were synthesized through a procedure recently reported by our group.[9] Briefly, the impregnated samples were first exposed to propionic acid vapors at 80 °C for 15 h and then thermally treated under N_2 at 280 °C for 2 h. The resulting inorganic core/carbon shell composites are denoted as CS−X, X being the chemical formula for the encapsulated compound as deduced by means of X-ray analysis.

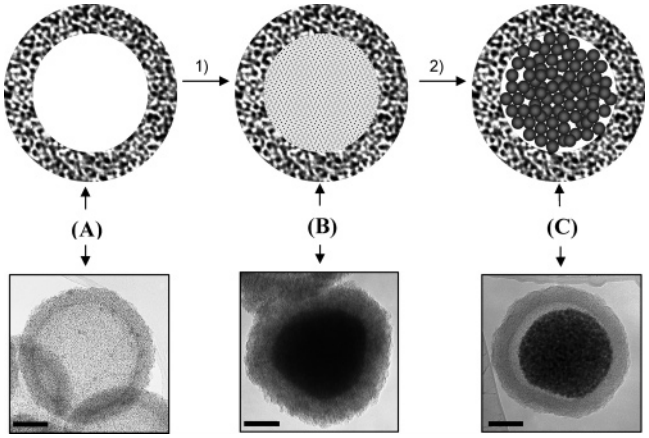

Figure 1. Illustration of the synthesis procedure. (A) Carbon capsule; (B) carbon capsule loaded with the inorganic precursor; (C) inorganic nanoparticles encapsulated within the mesoporous carbon shell. (1) Filling of the carbon capsule with the inorganic precursor; (2) conversion of the inorganic precursor into inorganic nanoparticles. Bar scale = 100 nm.

Enzyme Immobilization. Around 10 mg of the CS−Fe_xO_y-20 composite was dispersed at room temperature in 10 mL of lysozyme (Aldrich) solution (initial concentration: 0.5 mg lysozyme$\cdot g^{-1}$, pH 11 buffer solution) in a closed vessel to avoid evaporation. To evaluate the amount of enzyme immobilized, the concentration of lysozyme in the solution was periodically monitored by means of a UV−vis spectrophotometer (Shimadzu UV-2401PC) using UV absorption at 280 nm.

Characterization. X-ray diffraction (XRD) patterns were obtained on a Siemens D5000 instrument operating at 40 kV and 20 mA, using Cu Kα radiation. The morphology of the powders was

(6) (a) Liz-Marzan, L. M.; Giersig, M.; Mulvaney, P. *Langmuir* **1996**, *12*, 4329. (b) Lu, Y.; Yin, Y. D.; Li, Z. Y.; Xia, Y. A. *Nano Lett.* **2002**, *2*, 785. (c) Tartaj, P. *Chem. Phys. Chem.* **2003**, *4*, 1371. (d) Sun, X. M.; Li, Y. D. *Angew. Chem., Int. Ed.* **2004**, *43*, 597. (e) Sun, X. M.; Li, Y. D. *Langmuir* **2005**, *21*, 6019. (f) Zhao, W.; Gu, J.; Zhang, L.; Chen, H.; Shi, J. *J. Am. Chem. Soc.* **2005**, *127*, 8916. (g) Kim, J.; Lee, J. E.; Lee, J.; Ju, J. H.; Kim, B. C.; Ang, K.; Hwang, Y.; Sin, C. H.; Park, J. G.; Hyeon, T. *J. Am. Chem. Soc.* **2006**, *128*, 688. (h) Ge, J. P.; Xu, S.; Zhuang, J.; Wang, X.; Peng, Q.; Li, Y. D. *Inorg. Chem.* **2006**, *45*, 4922. (i) Fang, H.; Ma, C. Y.; Wan, T. L.; Zhang, M.; Shi, W. H. *J. Phys. Chem.* C **2007**, *111*, 1065.
(7) Tartaj, P.; González-Carreño, T.; Serna, C. J. *Adv. Mater.* **2001**, *13*, 1620.
(8) Buchel, G.; Unger, K. K.; Matsumoto, A.; Tsutsumi, K. *Adv. Mater.* **1998**, *10*, 1036.
(9) (a) Fuertes, A. B.; Tartaj, P. *Chem. Mater.* **2006**, *18*, 1675. (b) Fuertes, A. B.; Tartaj, P. *Small* **2007**, *3*, 275.

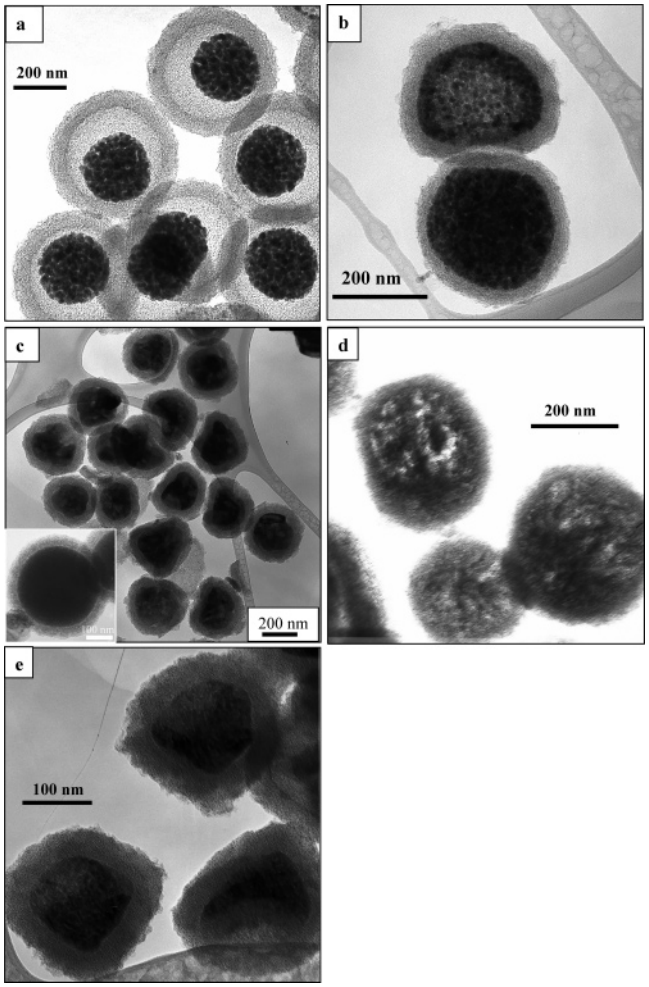

Figure 2. TEM images obtained for the core/shell nanocomposites. (a) CS−Fe_xO_y, (b) CS−$CoFe_2O_4$, (c) CS−$LiCoPO_4$, (d) CS−NiO, (e) CS−Cr_2O_3. The inset in (c) shows a spherical capsule after it has been filled with the inorganic precursor.

examined by scanning (SEM, Zeiss DSM 942) and transmission (TEM, JEOL-2000 FXII) electron microscopy. Nitrogen adsorption and desorption isotherms were performed at −196 °C in a Micromeritics ASAP 2010 volumetric adsorption system. The BET surface area was deduced from the analysis of the isotherm in the relative pressure range of 0.04−0.20. The total pore volume was calculated from the amount adsorbed at a relative pressure of 0.99. The PSD was calculated by means of the Kruk−Jaroniec−Sayari method.[10] The magnetization curves (up to a field of 5 T) of the samples were recorded on a vibrating sample magnetometer (MLVSM9 MagLab 9 T, Oxford Instrument). The saturation magnetization (M_s) and coercivity field values (H_c) were obtained from the magnetization curves. In particular, M_s values were derived from $1/H$ extrapolation at high fields.

Results and Discussion

The procedure employed to obtain the core/shell nanocomposites is illustrated in Figure 1. Two steps are required for this objective: (1) the macroporous core of the carbon capsules is loaded with an inorganic precursor by means of the dropwise technique; (2) the infiltrated compound is converted into the inorganic nanoparticles by means of chemical and thermal treatments. The hollow cores of the carbon capsules impregnated following the dropwise technique are completely filled by the inorganic precursor. This is clearly shown in the TEM image B in Figure 1 obtained for a carbon capsule filled with iron(III) nitrate. Moreover, TEM inspection of this impregnated sample shows that the inorganic compound is mainly deposited in the macroporous core. This suggests that the driving force behind the filling of the hollow core of the carbon capsules by the inorganic compound solution is the capillary motion through the mesopores of the carbon shell. Once the inorganic precursor is loaded into the carbon capsule, it can be converted into inorganic nanoparticles by combining the appropriate chemical and thermal treatments (see the Experimental Section for details). The TEM image C in Figure 1 shows an example of a carbon capsule loaded with inorganic nanoparticles of magnetic iron oxide spinel. These nanoparticles form agglomerates that exhibit a blackberry-like morphology.

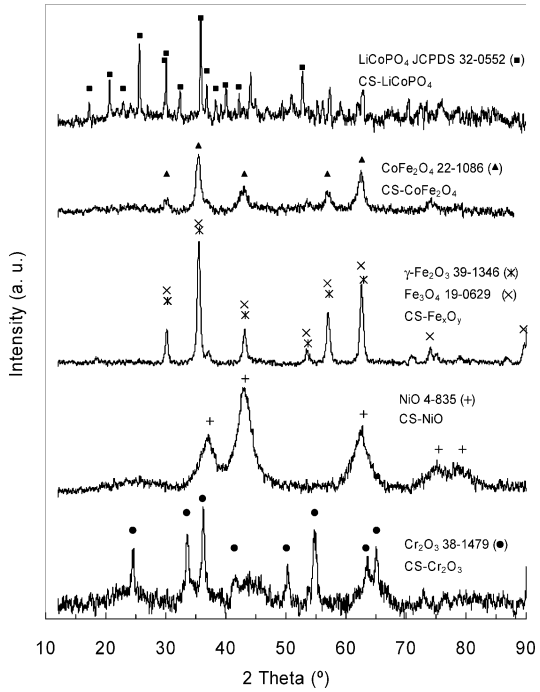

Figure 3. XRD patterns obtained for the of the inorganic core/mesoporous carbon shell nanocomposites.

We applied this synthetic method to the encapsulation of different types of inorganic nanoparticles—Fe_xO_y, $CoFe_2O_4$, $LiCoPO_4$, NiO, and Cr_2O_3—within a mesoporous carbon shell. Typical TEM images obtained for these composites are shown in Figure 2. They reveal that in all cases the inorganic phase occupies the hollow core of the carbon capsule. We also observed that, in some cases, the spherical morphology of the carbon capsules is partially lost (i.e., CS−$LiCoPO_4$ in Figure 2b). The inset in Figure 2c showing a spherical capsule after it has been filled with the inorganic precursor clearly indicates that the capsules are deformed during heat/chemical treatment. Moreover, it can be seen that for many particles the encapsulated inorganic compound does not completely fill the core of the capsule (see Figure 2, parts a and d) because of shrinkage resulting from the transformation of the inorganic precursor to the final inorganic phase. This is clear from a comparison of the TEM images B and C in Figure 1.

(10) Kruk, M.; Jaroniec, M.; Sayari, A. *Langmuir* **1997**, *13*, 6267.

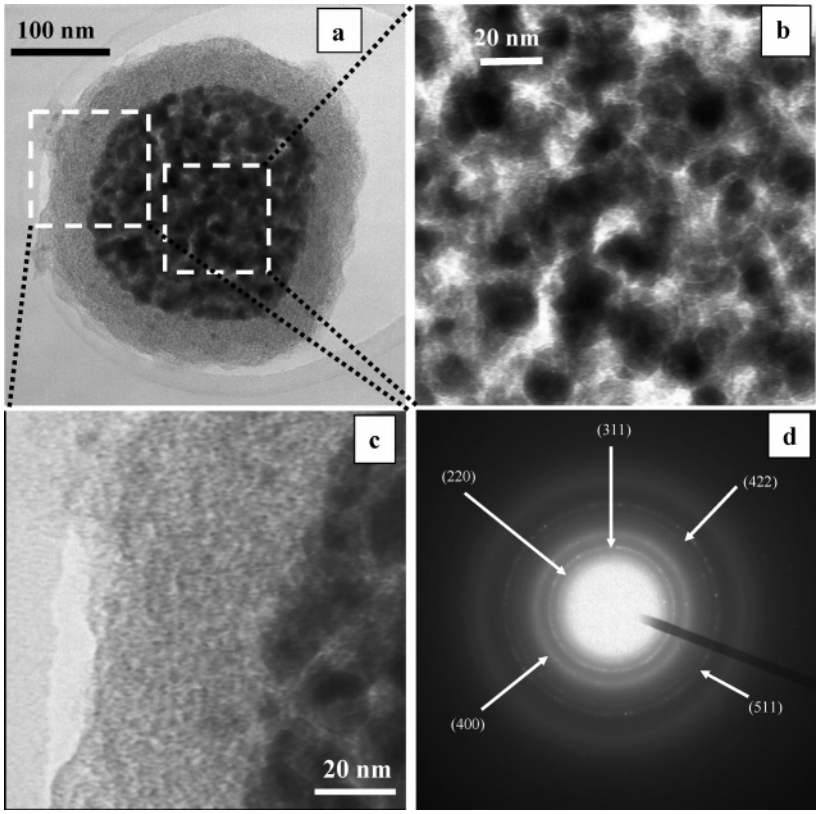

Figure 4. TEM images of (a) carbon capsule containing iron oxide nanoparticles with spinel structure (CS−Fe_xO_y); (b) high-magnification image of the inorganic core; (c) high-magnification image of the porous carbon shell; (d) selected-area electron diffraction (SAED) pattern for the Fe_xO_y encapsulated inorganic nanoparticles.

Evidence for the formation of encapsulated inorganic phases was obtained by XRD analysis. The XRD patterns shown in Figure 3 indicate that the encapsulated inorganic phases are well-crystallized. The sizes of the crystallites deduced by applying the Scherrer equation to the main peak of the XRD patterns are listed in Table 1. In general, the encapsulated inorganic phase consists of an agglomeration of nanoparticles. This is clear from the high-magnification TEM image in Figure 4b, which was obtained from a CS−Fe_xO_y particle (Figure 4a). The size of these iron oxide ferrite nanoparticles deduced from the TEM image is in agreement with the size calculated by means of XRD. The carbon shell encapsulating the inorganic phase hardly contains deposited nanoparticles. This is clearly evidenced by Figure 4c which shows a high-magnification image of the carbon layer of a carbon capsule filled by iron oxide nanoparticles (CS−Fe_xO_y sample). It can be seen that there is a sharp boundary between the encapsulated inorganic phase and the porous carbon shell (∼50 nm in thickness). The selected-area electron diffraction (SAED) pattern obtained for the CS−Fe_xO_y composite confirms the crystallinity of encapsulated iron oxide spinel nanoparticles (Figure 4d).

The nitrogen sorption isotherms obtained from these nanocomposites (see Figure S1 in the Supporting Information) show that these materials have a well-developed porosity, which can be assigned almost exclusively to the porous carbon layer. In fact, the contribution of the inorganic phase to the overall textural properties is negligible. These materials exhibit large BET surface areas and high pore volumes (Table 1). Moreover, the porosity is made up of mesopores in the 2−2.5 nm range as illustrated by the pore size distributions represented in Figure S1/insets (Supporting Information). Obviously, a small fraction of inorganic nanoparticles is deposited in the porous carbon shell. In consequence, a reduction in the textural properties of the composite in comparison with the nonimpregnated carbon capsules is expected. The importance of this reduction is analyzed for the CS−Fe_xO_y sample, for which the BET surface area and pore volume values, expressed on a carbon mass basis (normalized to carbon content), are 1180 $m^2 \cdot g^{-1}$ C and 1 $cm^3 \cdot g^{-1}$ C, respectively. These values are substantially lower than those obtained for the empty carbon capsules, 1870 $m^2 \cdot g^{-1}$ and 2.0 $cm^3 \cdot g^{-1}$, respectively. However, although this is a reduction, the above results show that after the encapsulation of inorganic phase the carbon shell still retains a large BET surface area and a high pore volume. Consequently, a significant fraction of its porosity remains unobstructed. This is important for applications that require the rapid transport of species through the carbon shell as, for example, when the encapsulated materials are either catalysts or electroactive substances.

In order to demonstrate the potential of the core/shell magnetic nanocomposites, we examined their ability to immobilize enzymes. For this experiment, the macroporous core of the composite contained around 20 wt % of iron oxide ferrite nanoparticles (this sample was denoted as CS−Fe_xO_y-20). As the model enzyme we used lysozyme, which has been extensively investigated for this purpose in other porous materials (silica and carbon).[11] The SEM image in Figure 5a reveals that this core/shell composite consists of highly uniform spherical particles with diameters of around 350 nm. The TEM image in Figure 5a (inset) shows that for this

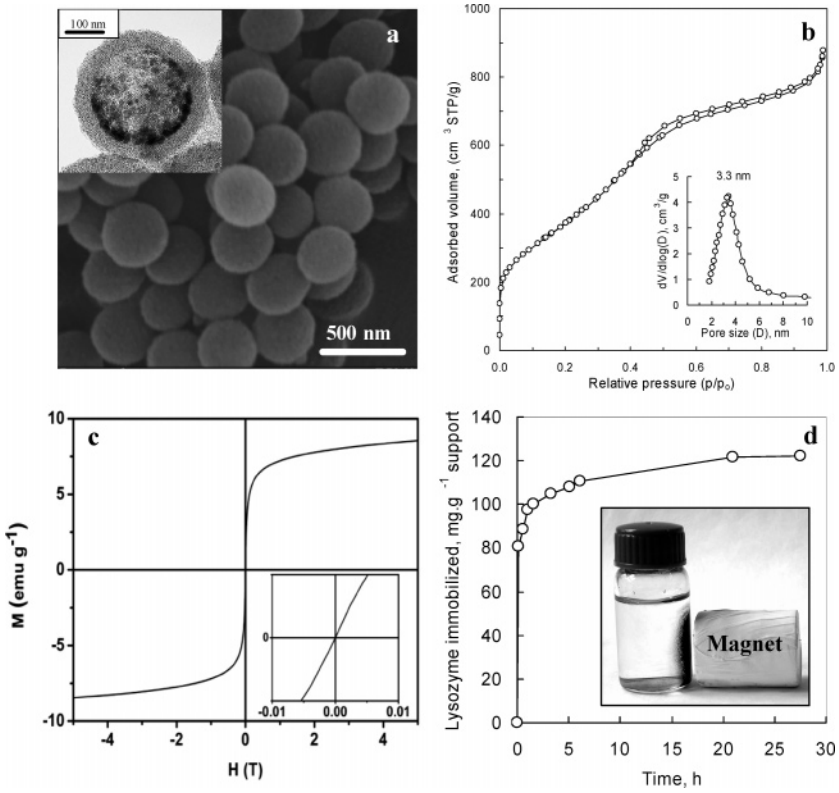

Figure 5. (a) SEM and TEM (inset) images of the CS−Fe_xO_y-20 composite. (b) Nitrogen sorption isotherm and pore size distribution (inset) of the CS−Fe_xO_y-20 sample. (c) Field-dependent magnetization at 300 K of CS−Fe_xO_y-20 (inset: low-field magnetization). (d) Immobilization of the lysozyme on the CS−Fe_xO_y-20 nanocomposite (inset: magnetic separation of the CS−Fe_xO_y-20 particles loaded with lysozyme).

material the encapsulated iron oxide ferrite nanoparticles occupy only a fraction of the volume of the hollow core because of the relatively low amount of inorganic phase encapsulated. The capsule was only partially filled in order to leave some free space inside the capsule. In recent experiments with carbon capsules we observed that an important fraction of immobilized biomolecules is occupying the macroporous core.[12] Then, in our opinion, the partial loading of the capsule by the inorganic phase can permit an increase of the storage capacity of the system. The size of the encapsulated iron oxide ferrite nanoparticles was around 8−9 nm, as deduced from the TEM image (Figure 5a, inset) and from the XRD pattern (Figure S2 in the Supporting Information). The CS−Fe_xO_y-20 material exhibits a large BET surface area (1370 $m^2 \cdot g^{-1}$) and a high pore volume (1.36 $cm^3 \cdot g^{-1}$) as can be inferred from the nitrogen sorption isotherm (Figure 5b). The pore size distribution (Figure 5b, inset) shows that the porous carbon shell of this composite has a porosity made up of mesopores (∼3.3 nm). As well as needing to have a large enough load of magnetic material, it is desirable that the samples display reversible magnetic behavior (interacting or noninteracting superparamagnetic behavior) at room temperature.[6c,13] We, therefore, recorded the room-temperature magnetization curve for the CS−Fe_xO_y-20 nanocomposite (Figure 5c). The sample displayed reversible magnetic behavior (zero coercivity field, see Figure 4c/inset) with a saturation magnetization value of 9.5 emu·g^{-1}. Figure 5d shows the immobilization of the lysozyme on the CS−Fe_xO_y-20 nanocomposite. This was carried out at pH 11 close to the isolelectric point of the lysozyme (∼11). It can be seen that around 70% of the enzyme loading is achieved within the first 10 min. The amount of lysozyme immobilized after 24 h is about 122 mg lysozyme·g^{-1} support. In terms of carbon basis the saturation loading is about 153 mg lysozyme·g^{-1} C, which is close to the value reported by Vinu et al., under similar conditions (pH = 11), for templated mesoporous carbons.[11b] These results prove that these nanocomposites have a high capacity for immobilizing enzymes. What is more, the support containing the immobilized lysozyme can be captured by means of a simple magnet, which demonstrates that the enzyme can be easily separated (see Figure 5d, inset).

Conclusions

In summary, we have described a procedure for successfully fabricating core/shell nanocomposites (diameter ∼400 nm) made up of inorganic nanoparticles confined within a mesoporous carbon capsule (shell thickness ∼50 nm). This synthetic strategy has a great versatility as demonstrated in this paper through the encapsulation of a wide variety of inorganic materials (Fe_3O_4/γ-Fe_2O_3, $CoFe_2O_4$, $LiCoPO_4$, NiO, and Cr_2O_3). A relevant characteristic of these core/shell composites is that, whereas the inner macroporous core can be almost completely filled by nanoparticles, the porosity of the carbon shell hardly contains deposited nanoparticles. This feature makes these composites suitable for a wide range

(11) (a) Lei, J.; Yu, C.; Zhang, L.; Jiang, S.; Tu, B.; Zhao, D. *Microporous Mesoporous Mater.* **2004**, *73*, 121. (b) Vinu, A.; Miyahara, M.; Ariga, K. *J. Phys. Chem. B* **2005**, *109*, 6436. (c) Wang, Y.; Caruso, F. *Chem. Mater.* **2005**, *17*, 953.
(12) Fuertes, A. B.; Valdés-Solís, T.; Sevilla, M.; Tartaj, P. Unpublished results, 2007.
(13) (a) Tartaj, P.; González-Carreño, T.; Serna, C. J. *Langmuir* **2002**, *18*, 4556. (b) Tartaj, P. *Curr. Nanosci.* **2006**, *2*, 43.

of applications such as high-performance catalysts, materials for energy storage application (i.e., Li-ion batteries), or advanced adsorbents with novel functionalities (magnetic). We have proved that a large amount of enzyme (lysozyme) can be immobilized in a core/shell composite containing iron oxide ferrite nanoparticles (20 wt %) and that this material can be easily manipulated by means of an external magnetic field.

Acknowledgment. The financial support for this research provided by the MCyT (MAT2005-00262, MAT2005-03179, NANO2004-08805-C04-01) is gratefully acknowledged.

Supporting Information Available: Figures S1 and S2 (PDF). This material is available free of charge via the Internet at http://pubs.acs.org.

CM071713K